Investigating the Potential for a Milky Way Radio Halo

Nitika Yadlapalli[1], Vikram Ravi[1]
[1]*Department of Astronomy, California Institute of Technology*

This work seeks to investigate the source of the excess radio background emission detected by balloon experiment, ARCADE 2. While similar experiments in the past used a plane-parallel slab model to explain the galatic forground, we use a disk and halo model to test for the existence of a galactic radio halo. Such a halo might form via cosmic rays from the plane of the galaxy diffusing out along magnetic field lines, and would leave a specific geometric signature in the sky brightness. Fits to all-sky maps in both image space and spherical harmonics space were attempted using Python packages `emcee` and `healpy`, though the presence of bright galactic features makes those results inconclusive. We also fit to data from another experiment, TRIS, which measures sky brightness along a single declination strip. Both of these techniques show preliminary evidence for the existence of a halo, though further study is required to conclusively state the physical meaning of these results.

I. INTRODUCTION

The radio sky can be written as the sum of three components: galactic foreground, extragalctic sources, and the CMB.

$$T_{sky} = T_{gal} + T_{EG} + T_{CMB} \tag{1}$$

Thus, experiments interested in measurements pertaining to the CMB must take care to accurately subtract off contributions from extragalactic sources and the galaxy. A balloon experiment from 2006, the Absolute Radiometer for Cosmology, Astrophysics and Diffuse Emission (ARCADE 2), sought to measure the deviations from the CMB's blackbody spectrum at frequencies lower than other CMB missions, like *COBE*/FIRAS (Fixsen et al. 2011). ARCADE 2 observed in five frequency bands (3, 8, 10, 30, and 90 GHz) and made use of an external blackbody calibrator in order to characterize instrumental effects. Galactic emission was modelled with a plane-parallel slab model, where brightness temperature, T_b, is a linear function of $csc(b)$ where b is galactic latitude (Kogut et al. 2011). After applying this model for the galaxy, and subtracting off brightness temperature contributions from the CMB and extragalactic sources, the ARCADE 2 team finds approximately 0.5 K excess temperature of unknown origin (Seiffert et al. 2011). Several theories have been proposed for this excess, many of which are summarized in Singal et al. (2018), but the one of interest in this report is the possibility of a galactic synchrotron halo.

The theory for a galactic radio-emitting halo dates back as far as the 1960s. Ginzburg & Syrovatsky (1961) suggest the existence of a galactic halo composed of cosmic rays with a radius of around 10 kpc. They believe cosmic rays originate in the disk and travel along magnetic field lines into the halo. As the halo is predicted to be spherical/ellipsoidal and isotropic, this implies disordered magnetic fields in the disk. As long as the particles diffuse out of the disk faster than their synchrotron lifetimes, a synchrotron-emitting halo would be observed. One method of testing the existence of a halo would be to attempt to fit a disk/halo geometry to current all-sky maps. Such an analysis of modelling the sky using two spheroids, one for the disk and one for the halo, was done by Subrahmanyan & Cowsik (2013). A variation on that analysis is performed in this study as well.

Similar to ARCADE 2, another absolutely calibrated experiment called TRIS observed a circle on the sky at a constant declination of 42° and ν = 0.6, 0.82, and 2.5 GHz (Zannoni et al. 2008).

Rather than trying to create a model of the galaxy, the TRIS team came up with a method of subtracting off the galactic component from the uniform component just using their data. First, they generate a TT plot for two different frequencies. In this case, they plotted T_b(0.82 GHz) vs. T_b(0.6 GHz). From this plot, they find regions of two distinct spectral indices which they can use to find a galactic temperature at a reference right ascension. Then, they use this reference temperature to calculate the temperature of the galaxy at every right ascension using equation 2. A derivation of this is given in Gervasi et al. (2008) and Tartari et al. (2008). The TRIS team reports no excess background temperature.

$$T_{gal}\left(\nu,\alpha_1\right) = \left[T_{sky}\left(\nu,\alpha_1\right) - T_{sky}\left(\nu,\alpha_{ref}\right)\right] + T_{gal}\left(\nu,\alpha_{ref}\right) \tag{2}$$

A radio halo in our own galaxy could give us insight into the formation mechanisms of similar halos observed in other galaxies.The Continuum Halos in Nearby Galaxies, an EVLA Survey (CHANG-ES), for example aims to study extragalactic radio halos. They find that many of the edge-on spiral galaxies they observed exhibited halos of magnetic fields and cosmic rays (Wiegert et al. 2015). Should evidence of such a halo be found for the Milky Way as well, we would be in a unique place to study the origins of radio halos.

This report is organized as follows. First, we discuss our models of the galactic foreground as well as our calculations for brightness temperature of extragalactic sources. We then discuss fitting model parameters to all-sky maps and the limitations of those analyses. We then discuss similar analyses carried out for data taken by TRIS. A brief discussion of results is given for each section.

II. METHODS

A. Disk and Halo Models

In order to fit disk and halo models to currently available observations, we first needed to come up with models calculated from the perspective of the earth. By assuming an isotropic emissivity and by calculating the line of sight distance through the disk and halo, we can calculate the predicted brightness temperature from the model in all directions via equations 3 - where I_ν is the specific intensity, j_ν is the emission coefficient of the disk/halo, and D is the line of sight distance through the disk/halo - and 4, the Rayleigh-Jeans limit of the Planck function.

$$I_\nu = j_\nu D \tag{3}$$

$$T_b = \frac{I_\nu c^2}{2k\nu^2} \tag{4}$$

We initially assumed a cylindrical model for the galactic disk. The line of sight distance would be dependent on the radius of the cylinder, R_{disk}, the height, h_{disk}, distance from the galactic center, d, and galactic longitude and latitude, l and b. In some instances, we found a spheroidal model for the disk to be preferabe to the cylindrical one. For the spheroidal models, we assume that R_{disk} represents the semi-major axis while h_{disk} represents the semi-minor axis. For comparison, an example for each model, given the same geometric values and emissivity, is shown in Fig 1. For the halo, we assume a spherical geometry. An example of this model is shown in Figure 2.

B. Extragalactic Temperature Contribution

In order to calculate the total brightness contributed by extragalactic sources, several models covering source counts for different brightness ranges were combined. Source counts in the range of

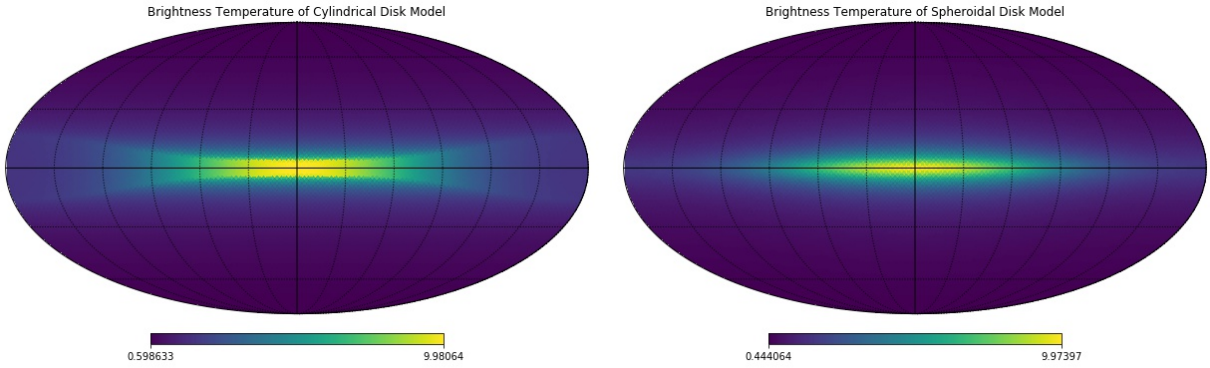

Figure 1. Two examples of models for a galactic disk. On the left is a cylindrical model while on the right is a spheroidal model

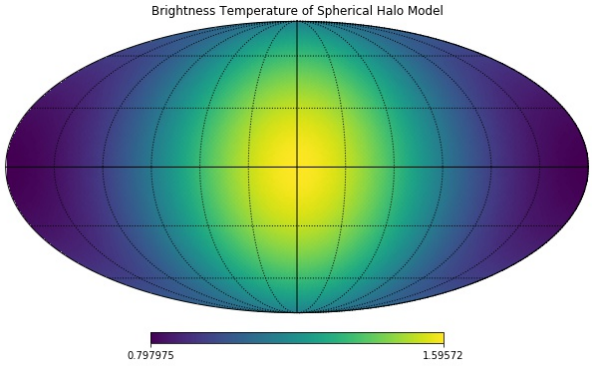

Figure 2. An example of a model for a galactic halo.

0.05 - 1000 mJy can be modelled by the sixth order polynomial described by equation 5 (Hopkins et al. 2003).

$$log\left(\frac{dN/dS}{S^{-2.5}}\right) = -0.008x^6 + 0.057x^5 - 0.121x^4 - 0.049x^3 + 0.376x^2 + 0.508x + 0.859 \quad (5)$$

$$x = log\left(\frac{S}{mJy}\right)$$

In the range of $0.011 - 44$ mJy, Smolčić et al. (2017) reports specific values for $\frac{dN/dS}{S^{-2.5}}$ at various sky brightnesses. Finally, in the range of $S < 10$ μJy, Condon et al. (2012) predicts that the source counts at 3.02 GHz are described by equation 6.

$$\frac{dN}{dS} = 9000S^{-1.7}\ Jy^{-1}\ sr^{-1} \quad (6)$$

As these equations describe source counts at various frequencies, we need to use equation 7 to transform S into the frequency of our choice, where the spectral index is $\alpha = -0.7$.

$$S_f = S_i \left(\frac{\nu_f}{\nu_i}\right)^{\alpha} \tag{7}$$

Once all of the brightnesses are at a consistent frequency, equation 8 describes how to calculate the final integrated brightness temperature. A plot representing the differential temperature is shown in Figure 3.

$$T_b = \int \left(\frac{dT}{dS}\right) dS \; = \int \left(S\frac{dN}{dS}\right) \frac{c^2}{2\nu^2 k} dS \tag{8}$$

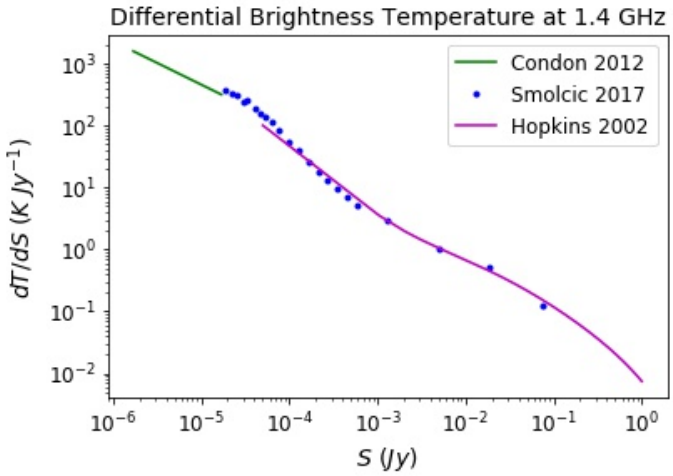

Figure 3. Differential brightness temperature plotted as a function of source brightness at 1.4 GHz

III. RESULTS AND DISCUSSION

A. Fitting to Images

Our first attempt to fit a disk+halo galaxy model to an all-sky radio image was to a 1.4 GHz map downloaded from NASA's LAMBDA database. In order to assess the fit, we need to analyze the residuals, calculated in equation 9, where the T_{bkg} is a free parameter meant to represent any excess uniform emission.

13

$$T_{residual}(l,b) = T_{sky}(l,b) - (T_{disk}(l,b) + T_{halo}(l,b)) - T_{extragalactic} - T_{CMB} - T_{bkg} \tag{9}$$

For an ideal model, the sky temperature minus the model temperature should just leave Gaussian noise. In reality, it is impossible for our rudimentary models to subtract precise structure, so we will be left with more positive residuals than negative. The residuals should follow a right-tailed distribution, where the negative residuals resemble half a Gaussian and the positive residuals include residual emission caused by specific features, such as the loops and spurs. So, to assess the fit, we measure the Gaussianity of the negative residuals with a Kolmogorov-Smirnov test (KS test). This

14

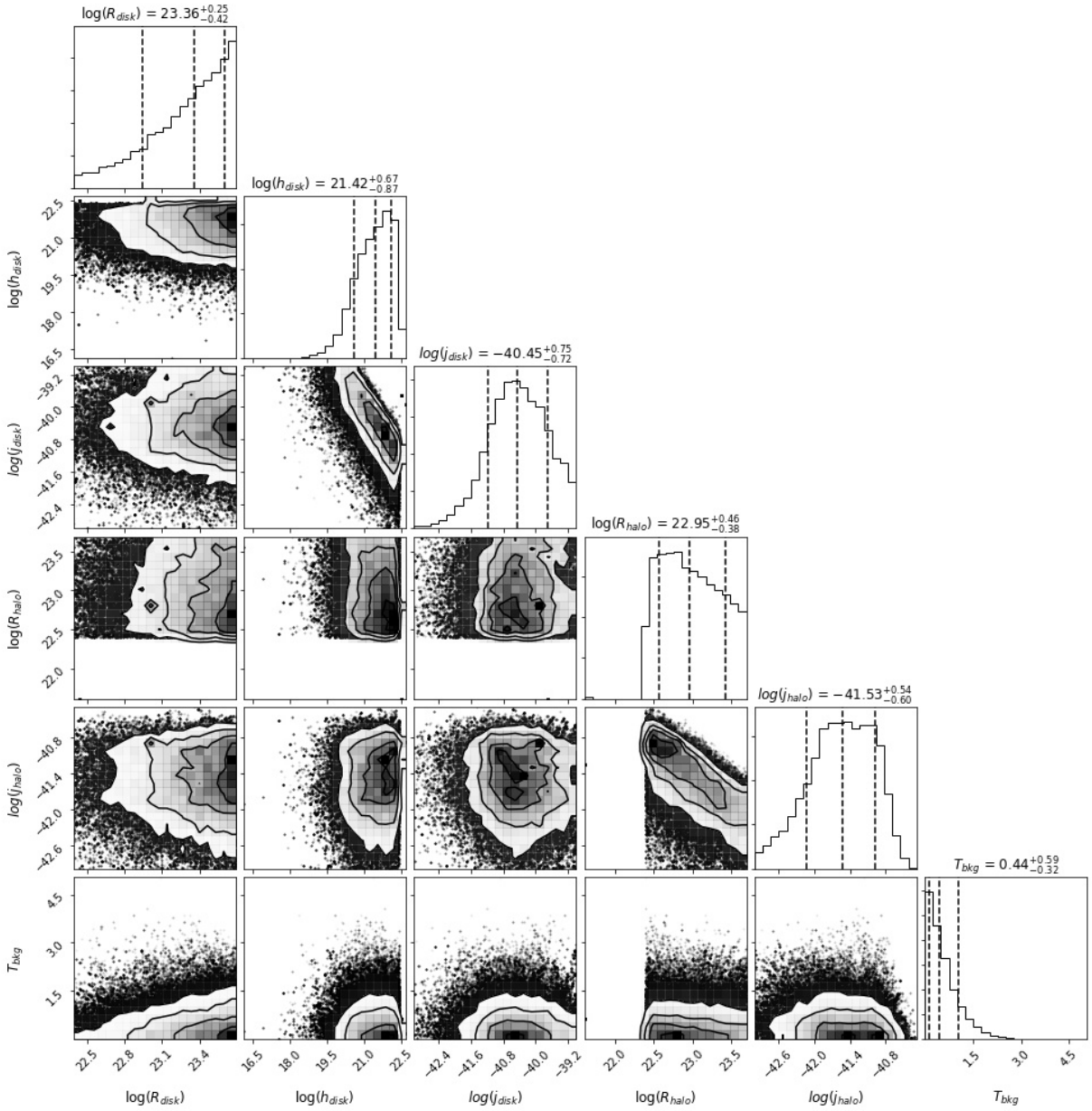

Figure 4. Corner plot showing the results from the MCMC analysis of the 1.4 GHz all sky map assuming a disk, halo, and uniform background model for the galaxy.

statistical test measures the maximum distance between the cummulative distribution function of the residuals and an empirical distribution function (EDF). The larger this maximum distance, the lower the p-value of the test. In order to find the set of parameters that best represent the data, we perform an MCMC analysis, using Python package `emcee` (Foreman-Mackey et al. 2013), with the negative of the p-value of the KS test being the statistic we wish to minimize. This analysis involved six free parameters: R_{disk}, h_{disk}, j_{disk}, R_{halo}, j_{halo}, and T_{bkg}. As emission towards the galactic center is very bright, the central 20° of latitude were not included in the analysis. However, this led to a poor constraint on the best fit for R_{disk}. The results of the MCMC analysis also show the maximum likelihood of T_{bkg} is 0 K, indicating that there may be no excess emission

left unexplained after including a halo in the model of the galaxy. The resulting corner plot from the analysis is shown in Figure 4.

In a separate MCMC analysis of a disk and background only model (no halo), the Markov chain for background temperature showed a maximum likelihood around 0.6 K. This is fairly close to the 0.5 K excess reported by the ARCADE 2 team. The absence of this background in the analysis including contributions from the halo indicates some merit in the halo model, but further investigation is needed to confirm.

In addition to an attempt to fit the models in image space, a fit in spherical harmonics space was also attempted. Using Python package `healpy`'s spherical harmonics transforms, coefficients for the sky map and the models are computed. Then, the error in the coefficients is minimized to find the best fit using MCMC. Ultimately, fitting in both image space and spherical harmonics space was unsuccessful as the models that better subtracted bright features like loops and spurs, especially the North Galactic Spur, were preferred. An analysis that avoids this structure has better potential for success, thus, we attempt similar fits to the TRIS data.

B. Fitting to TRIS Data

The TRIS team observed the sky at a constant declination ($\delta = 42°$) and thus, were able to create plots of brightness temperature as a function of RA. They then used equation 2 to calculate the temperature of the galactic foreground at every RA. A plot showing the temperatures of the sky and galaxy together at 0.6 GHz is shown in Figure 5. We are now interested in fitting a disk and halo model to this data. The advantage of the TRIS dataset is that it avoids areas with large, bright features. As there are too few data points in the TRIS dataset to use the KS test as our test statistic, we instead use an integral of the absolute value of the residuals, as quantified by equation 10, as the statistic we wish to minimize. Two separate MCMC anaylses were performed, one with just a disk and one with a disk and a halo. It should be noted that in this analysis, a spheroidal disk was preferred to a cylindrical one.

$$T_{res} = T_{gal} - (T_{disk} + T_{halo}) \tag{10}$$

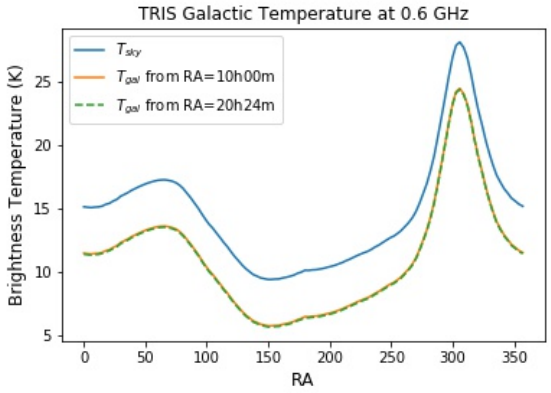

Figure 5. Temperature of sky and galactic foreground as a function of RA, as measured by TRIS at 0.6 GHz. Galactic temperature is calculated using two separate reference locations. As expected, both references yield the same values for T_{gal}

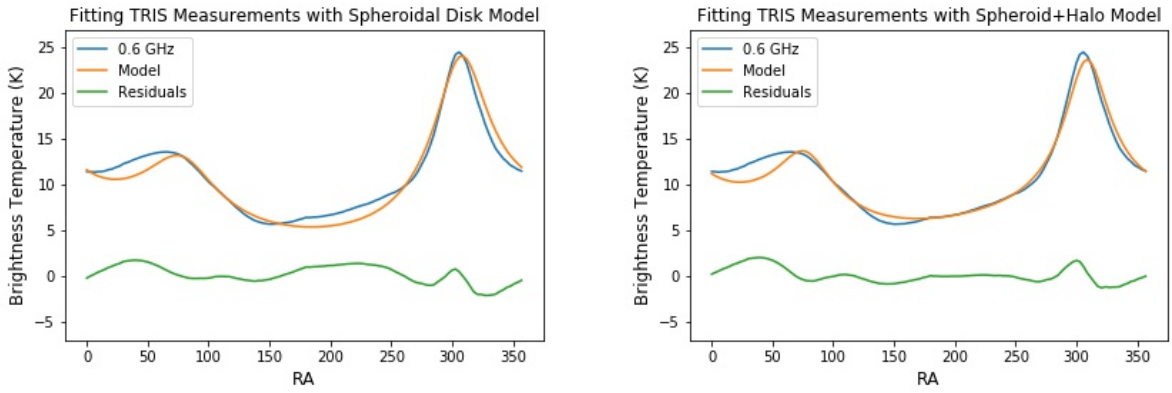

Figure 6. Residuals of the best fits, as calculated by the MCMC analysis, for a disk only model (left) and disk+halo model (right).

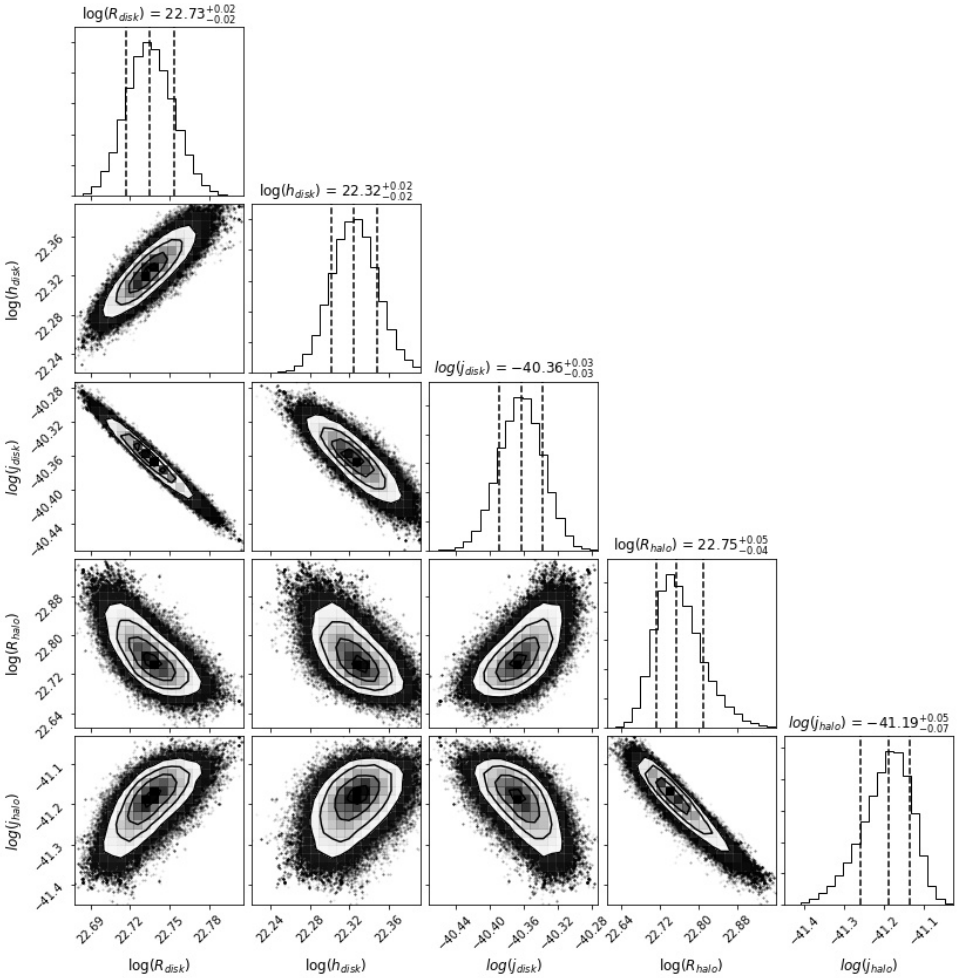

Figure 7. Corner plot showing the results from the MCMC analysis of the 0.6 GHz TRIS data, with the uniform background subtracted off, assuming a disk and halo model for the galaxy.

The highest likelihood model compared to the true sky temperature for both cases are shown in Figure 6. The peaks are reasonably well modelled in both cases, however the region between RA = 150° - 250° is only modelled accurately in the case of a disk+halo. The disk alone model fails to model the postitive slope in brightness temperature. The corner plot visualing the values of the parameters for the disk+halo model is shown in Figure 7. The highest likelihood values for R_{disk} and R_{halo} are about 17.4 kpc and 18.2 kpc respectively. The most likely value for h_{disk}, however, is around 0.85 kpc, indicating a fairly thick disk compared to the 0.3 kpc thickness predicted for the stellar disk. The thickness of the disk may be overpredicted, however, to compensate for extra brightness contributed by the Cygnus-X star forming region. Further work is necessary to interpret these results.

IV. CONCLUSION

This report presents results of using a galactic radio halo in attempts to explain the excess radio background reported by ARCADE 2. Fits to an all-sky 1.4 GHz map in image space showed the existence of a uniform background with a disk only model, which was not present in a disk+halo model. However, these results may be biased by the presence of bright features, such as the North Galactic spur, as the MCMC walkers tended towards parameter values that best modelled these features rather than overall galaxy structure. To avoid this, a similar analysis was done with the TRIS dataset, as the TRIS observing path avoids emission from the North Galactic Spur. Comparing the disk only model with the disk+halo model and the TRIS sky brightness data shows that the emission profile is best fit with the presence of the halo. These results are still preliminary, however, and statistical tests of model selection are necessary before any confident conclusions about the presence of the radio halo can be made.

REFERENCES

Condon, J. J., Cotton, W. D., Fomalont, E. B., et al. 2012, ApJ, 758, 23
Fixsen, D. J., Kogut, A., Levin, S., et al. 2011, ApJ, 734, 5
Foreman-Mackey, D., Hogg, D. W., Lang, D., & Goodman, J. 2013, PASP, 125, 306
Gervasi, M., Zannoni, M., Tartari, A., Boella, G., & Sironi, G. 2008, ApJ, 688, 24
Ginzburg, V. L., & Syrovatsky, S. I. 1961, Progress of Theoretical Physics Supplement, 20, 1
Hopkins, A. M., Afonso, J., Georgakakis, A., et al. 2003, arXiv e-prints, astro
Kogut, A., Fixsen, D. J., Levin, S. M., et al. 2011, ApJ, 734, 4
Seiffert, M., Fixsen, D. J., Kogut, A., et al. 2011, ApJ, 734, 6
Singal, J., Haider, J., Ajello, M., et al. 2018, PASP, 130, 036001
Smolčić, V., Novak, M., Bondi, M., et al. 2017, A&A, 602, A1
Subrahmanyan, R., & Cowsik, R. 2013, ApJ, 776, 42
Tartari, A., Zannoni, M., Gervasi, M., Boella, G., & Sironi, G. 2008, ApJ, 688, 32
Wiegert, T., Irwin, J., Miskolczi, A., et al. 2015, AJ, 150, 81
Zannoni, M., Tartari, A., Gervasi, M., et al. 2008, ApJ, 688, 12